Primljen / Received: 24.9.2014.
Ispravljen / Corrected: 17.2.2015.
Prihvaćen / Accepted: 31.3.2015.
Dostupno online / Available online: 10.7.2015.

Sector element for analysis of thick cylinders exposed to internal pressure and change of temperature

Authors:

Asma Bouzriba, MSc. CE
Bejaïa University, Algeria
Faculty of Civil Engineering
asmatfk@gmail.com

Prof. Cherif Bouzrira, PhD. CE
Jijel University, Algeria
Faculty of Civil Engineering
c_bouzrira@yahoo.fr

Scientific paper - Preliminary report

Asma Bouzriba, Cherif Bouzrira

Sector element for analysis of thick cylinders exposed to internal pressure and change of temperature

The strain-based approach for development of a sector in-plane finite element defined in the polar coordinate system is applied in the paper. The element is used for determining the plane state in elastic area. The developed element has three degrees of freedom in each node. The performance of this element was tested through analysis of thick cylinders exposed to internal pressure and change of temperature. The efficiency of the element was established, and the convergence of results for stresses and displacements of this element was shown to be faster compared to other elements.

Key words:
sector element, in-plane rotation, rigid body displacements, plane state, elasticity, temperature

Prethodno priopćenje

Asma Bouzriba, Cherif Bouzrira

Sektorski element za analizu debelih cijevi izloženih unutarnjem tlaku i promjeni temperature

U radu je primijenjen deformacijski pristup za razvoj sektorskog ravninskog konačnog elementa definiranog u polarnom koordinatnom sustavu. Element se koristi za određivanje ravninskog stanja u području elastičnosti. Razvijeni element ima tri stupnja slobode u svakom čvoru. Ponašanje ovog elementa ispitano je kroz analizu debelih cijevi izloženih unutarnjem tlaku i promjeni temperature. Utvrđena je efikasnost elementa i pokazano je da se primjenom ovog elementa postiže brža konvergencija rješenja pri izračunavanju naprezanja i pomaka nego u slučaju primjene drugih elemenata.

Ključne riječi:
sektorski element, rotacija u ravnini, pomaci krutih tijela, ravninsko stanje, elastičnost, temperatura

Vorherige Mitteilung

Asma Bouzriba, Cherif Bouzrira

Sektorelement zur Analyse starker Rohre unter Innendruck und Temperaturveränderung

In dieser Arbeit wird das Verformungsverfahren angewandt, um ein in Polarkoordinaten definiertes finites Sektorelement zur Analyse in der Ebene im elastischen Bereich zu entwickeln. Das eingeführte Element hat drei Freiheitsgrade in jedem Knotenpunkt. Das Verhalten des Elements wurde durch Analysen starker Rohre unter Innendruck und Temperaturveränderung erfragt. Die Effizienz des Elements konnte festgestellt werden und bei seiner Anwendung wurde eine schnellere Lösungskonvergenz bei der Berechnung von Spannungen und Verschiebungen erzielt, als bei dem Einsatz anderer Elemente.

Schlüsselwörter:
Sektorelement, Rotation in der Ebene, Verschiebung von Starrkörpern, Zustand in der Ebene, Elastizität, Temperatur

1. Introduction

The strain based approach has recently been cited in literature [1-3] with respect to the development of new finite elements, in which the displacement field can be obtained by strain integration. For plane stress problems, the simplest element shapes are obviously the triangle and rectangle with three or four nodes, respectively. However, for problems with curved boundaries, the use of triangular element means that the curved boundary has been approximated by a series of straight line segments. Furthermore, with some sophisticated elements being developed today, the error introduced by this approximation may well be the limiting factor in some solutions. Hence, the need for elements with curved boundaries is justified. The first attempt was made by Ergatoudis et al. [4] who introduced the isoperimetric approach. But, for problems with circular boundaries, it is convenient to use a sector element having a system of polar coordinates. Raju and Rao [5] developed a sector element having the only essential degrees of freedom by using polynomial expressions for the displacement field. More recently, Sabir et al. [6, 8], and Bouzrira et al. [9] used the strain-based approach to develop the sector element with two and three degrees of freedom per corner node.
The strain based approach is used in this paper to derive a new sector element in a system of polar coordinates possessing two translational degrees of freedom, and the inplane drilling rotation. The element is first tested for the case of bending of a curved bar. Once the results obtained showed a good performance, this element was used for the study of a thick cylinder under pressure and temperature constraints. The analysis of cylinder under temperature constraints has never been tested before using this approach.

2. Derivation of displacement function for sector element

For plane elasticity problems in a system of polar coordinates r and θ, the strain displacement equations are:

$$\varepsilon_r = \partial u / \partial r \tag{1.a}$$

$$\varepsilon_\theta = \frac{1}{r}\partial v / \partial\theta + u / r \tag{1.b}$$

$$\gamma_{r\theta} = \frac{1}{r}\partial u / \partial\theta + \partial v / \partial r - v / r \tag{1.c}$$

Where: ε_r, ε_θ and $\gamma_{r\theta}$ are direct and shearing strains, while u and v are displacements in the r and θ directions, respectively.
If these three strains are made equal to zero, we can integrate the resulting three differential equations to obtain the expressions for the displacement field corresponding to the rigid body movement. Hence:

$$u_R = \cos\theta\ a_1 + \sin\theta\ a_2 \tag{2. a}$$

$$v_R = -\sin\theta\ a_1 + \cos\theta\ a_2 + r\,a_3 \tag{2. b}$$

Where the constants a_1 and a_2 represent the rigid body translational movements in the r and θ directions, respectively, and a_3 represents the inplane rotation.

$$\varphi = 1/2\left(-\frac{1}{r}\partial u/\partial\theta + \partial v/\partial r + v/r\right) \tag{3}$$

Hence:

$$\phi_R = a_3 \tag{4}$$

The displacements function for this sector element should contain twelve independent constants. Three constants are required to represent the rigid body displacements. The remaining nine constants are available for expressing the displacements due to the straining of the element.

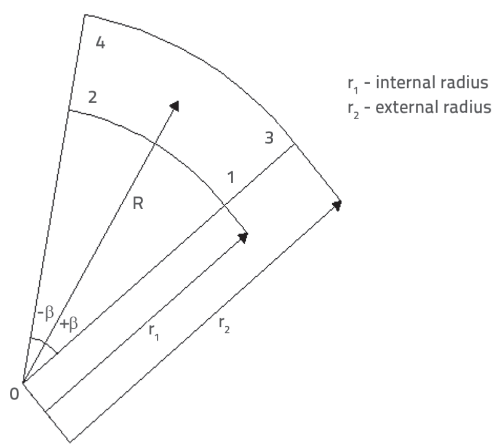

Figure 1. Sector element in polar coordinates

Hence:

$$\begin{cases} \varepsilon_r = a_4 + 2\,r\,a_6 + \theta\,a_{10} + 3\,r^2\,a_{11} \\ \varepsilon_\theta = a_5 + r\,a_6 - \dfrac{\theta r^3}{3}a_8 + \theta a_9 + r^2\,a_{11} \\ \gamma_{r\theta} = a_7 + \dfrac{\theta}{r}a_6 - \dfrac{r^3\theta^2}{2}a_8 + \dfrac{\theta}{r}a_{10} - 2ra_{12} \end{cases} \tag{5}$$

These strains given in Eqs. (5) satisfy the compatibility equation:

$$\frac{\partial^2\gamma_{r\theta}}{\partial r\,\partial\theta} - \frac{1}{r}\frac{\partial^2\varepsilon_r}{\partial^2\theta} - r\frac{\partial^2\varepsilon_\theta}{\partial^2 r} - 2\frac{\partial\varepsilon_\theta}{\partial r} + \frac{\partial\varepsilon_r}{\partial r} + \frac{1}{r}\frac{\partial\gamma_{r\theta}}{\partial\theta} = 0 \tag{6}$$

Eqs. (5) are then substituted into Eqs. (1) and the resulting differential equations are integrated to obtain the displacement functions as given below:

$$u_s = r\,a_4 + (1 + r^2)a_6 + (1 + \theta r)a_{10} + r^3 a_{11} \tag{7. a}$$

$$v_s = -r\theta a_4 + r\theta\,a_5 - \theta a_6 - \frac{r^4\theta^2}{6}a_8 + \frac{r\theta^2}{2}a_9 - \left(\frac{r\theta^2}{2} + \theta\right)a_{10} - r\log(r)\left(a_{10} - a_7\right) - 2r^2 a_{12} \tag{7. b}$$

$$\phi_s = -\theta a_4 + \theta a_5 - \frac{\theta}{2r}a_6 + \left(\frac{1}{2} + \log(r)\right)a_7 - \frac{5r^3\theta^2}{12}a_8 + \frac{\theta^2}{2}a_9 - \left(1 + \frac{\theta^2}{2} + \frac{\theta}{2r} + \log(r)\right)a_{10} - 3r\,a_{12} \tag{7. c}$$

The final displacement functions are obtained by adding the corresponding expressions for u, v and ϕ from Eqs. (2) and (4) to Eqs. (7).
The nodal displacement vector can be written in matrix form:

$$\{u_i\}=[C]\{A\} \tag{8}$$

where, {A} is the constant parameters vector and [C] is the transformation matrix as given in the Appendix.

$$\left[K^e\right]=\left[C^{-1}\right]^T\left[\iint[B]^T[D][B]\,r\,dr\,d\theta\right]\left[C^{-1}\right]=\left[C^{-1}\right]^T\left[K_0\right]\left[C^{-1}\right] \tag{9}$$

where, [D] is the rigidity matrix and [B] is the strain matrix.

$$\iint dr\,d\theta=\int_{-1}^{+1}\int_{-1}^{+1}\det[J]\,d\zeta\,d\eta \tag{10}$$

$$\left[K^e\right]=\left[C^{-1}\right]^T\left[\int_{-1}^{+1}\int_{-1}^{+1}r[B]^T[D][B]\det|J|\,d\zeta\,d\eta\right]\left[C^{-1}\right] \tag{11}$$

$$[B]=\begin{bmatrix} 0 & 0 & 0 & 1 & 0 & 2r & 0 & 0 & 0 & \theta & 3r^2 & 0 \\ 0 & 0 & 0 & 0 & 1 & r & 0 & -\frac{\theta r^3}{3} & \theta & 0 & r^2 & 0 \\ 0 & 0 & 0 & 0 & 0 & \frac{\theta}{r} & 1 & -\frac{\theta^2 r^3}{2} & 0 & \frac{\theta}{r} & 0 & -2r \end{bmatrix} \tag{12}$$

3. Thermoelasticity

For a two dimensional problem, the constitutive law of thermoelasticity for an isotropic material is:

$$\begin{Bmatrix}\sigma_r\\ \sigma_\theta\\ \tau_{r\theta}\end{Bmatrix}=[D]\begin{Bmatrix}\varepsilon_r\\ \varepsilon_\theta\\ \gamma_{r\theta}\end{Bmatrix}-[D_1]\,\alpha T\begin{Bmatrix}1\\ 1\\ 0\end{Bmatrix} \tag{13}$$

where:
T - temperature gradient
a - thermal expansion coefficient.

$$[D_1]=\frac{E}{1-v}\begin{bmatrix}1 & v & 0\\ v & 1 & 0\\ 0 & 0 & \frac{1-v}{2}\end{bmatrix} \tag{14}$$

$$\begin{Bmatrix}\varepsilon_r\\ \varepsilon_\theta\\ \gamma_{r\theta}\end{Bmatrix}=[B]\,[C]^{-1}\{U_i\} \tag{15}$$

Nodal force due to temperature gradient is given as follows:

$$\{F\}=\left[C^{-1}\right]^T\iint[B]^T[D_1]\,\alpha T\begin{Bmatrix}1\\ 1\\ 0\end{Bmatrix}r\,dr\,d\theta=\left[C^{-1}\right]^T\left[\int_{-1}^{+1}\int_{-1}^{+1}r[B]^T[D_1]\,\alpha T\begin{Bmatrix}1\\ 1\\ 0\end{Bmatrix}\det|J|\,d\xi\,d\eta\right] \tag{16}$$

For a steady state flow, if T_i is the temperature on the inner surface of the cylinder and the temperature on the outer surface is zero, the temperature T at any distance r from the centre is represented by the expression [10]:

$$T=\frac{T_i}{\log(b/a)}\log(b/r) \tag{17}$$

4. Numerical validation

To validate the level of accuracy and computational efficiency obtained with the developed element, several distinct examples for plane elasticity problems are presented.

4.1. Curved bar bending by applying force at the end

The first example is that of the two dimensional elasticity problem of a curved plate subjected to two equilibrating radial shearing forces, as shown in Figure 2. To obtain a set of comprehensive results, a considerable range of values of b/a is considered. From symmetry, only half of the annulus is analysed, and the results are compared with those obtained in references [7-9] and with the elasticity solution given by Timoshenko [10].

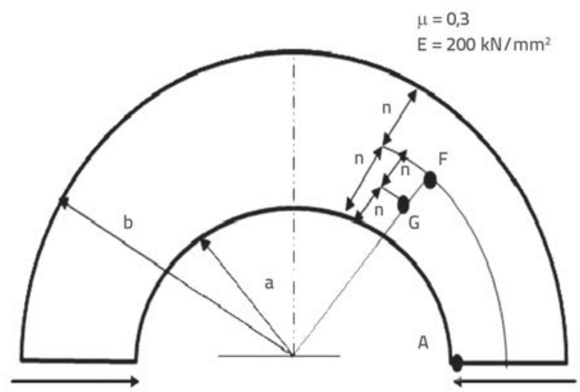

Figure 2. Annulus subjected to radial shear

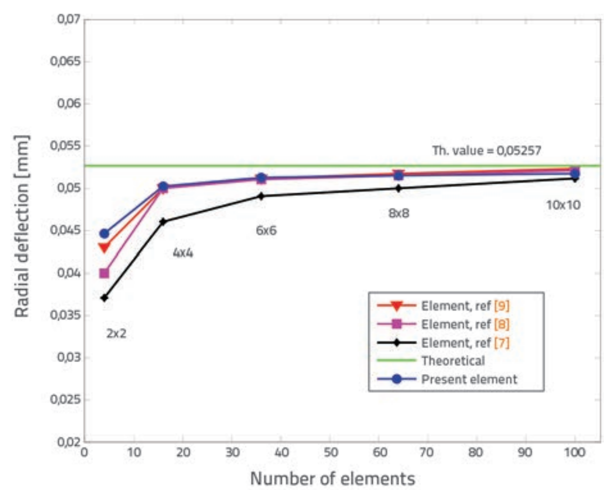

Figure 3. Convergence of u_A (b/a = 3)

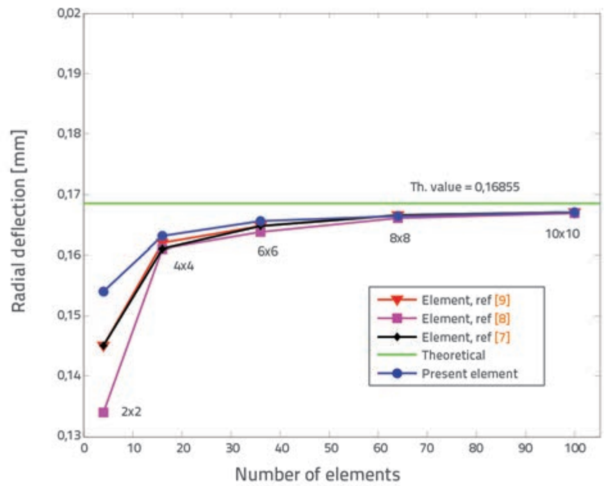

Figure 4. Convergence of u_A (b/a = 2)

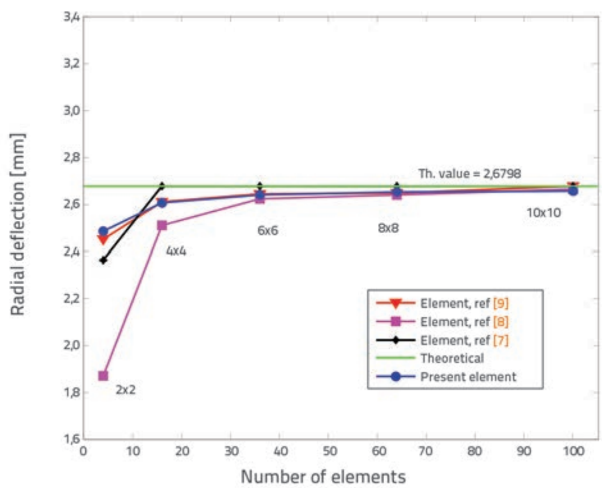

Figure 5. Convergence of u_A (b/a = 1.3)

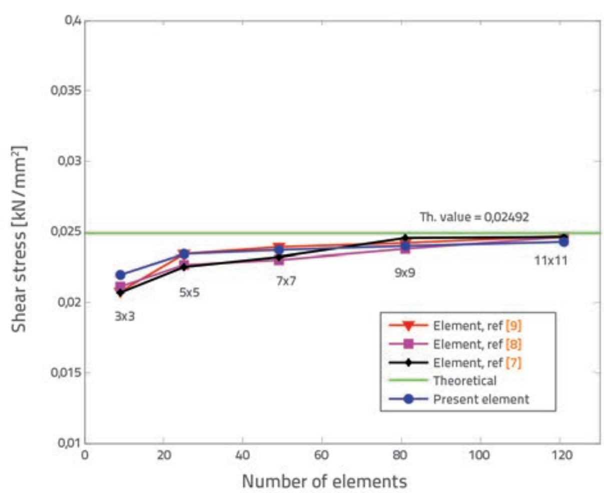

Figure 6. Convergence of shearing stress $\tau_{r\theta}$ at "F"

Figures 3, 4 and 5 give the convergence curves for the radial deflection at "A" (see Figure 2) for b/a = 3, 2 and 1.3, respectively. This result gives better results than the others elements.

Figures 6 and 7 give convergence curves for shearing and radial stresses at "F" (see Figure 2) for the case of b/a = 2. The present element was found to yield better results for radial stress when a coarse mesh is used.

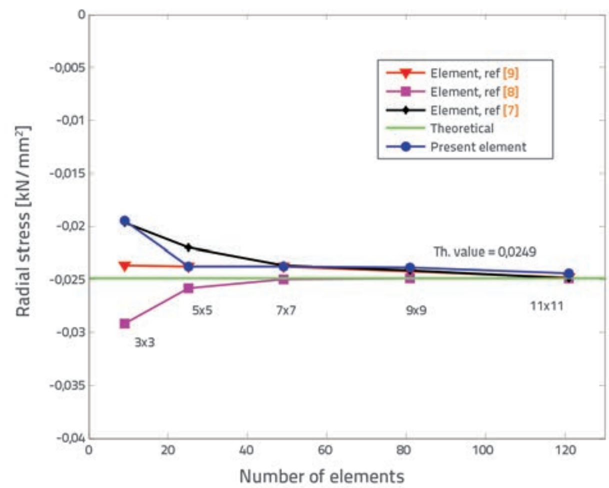

Figure 7. Convergence of σ_r at "F"

4.2. Study of thick cylinder subjected to internal pressure and temperature

The second problem to be considered is that of thick cylinder, as shown in Figure 8. Due to rotationally symmetric behaviour of the problem, only one quarter of the cylinder is considered for the finite element idealization.

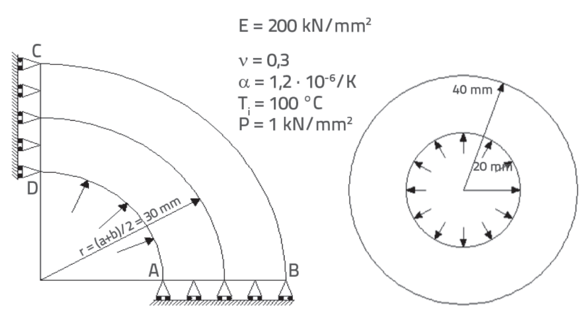

Figure 8. Thick cylinder subjected to internal pressure and temperature

4.2.1. Cylinder under pressure only

The computed results for the radial deflection, the radial and tangential stress at mid point along the radial section (r =30 mm), are presented in Figures 9 to 11, which show good agreement of the results obtained by the commercial program Cast3M [11].

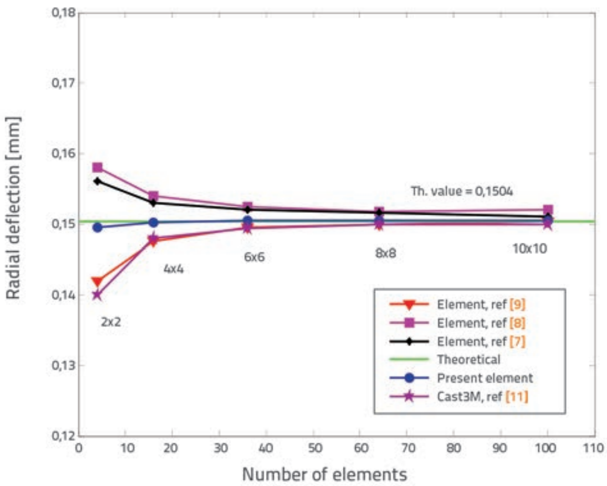

Figure 9. Convergence of *u* at *r* = 30 mm

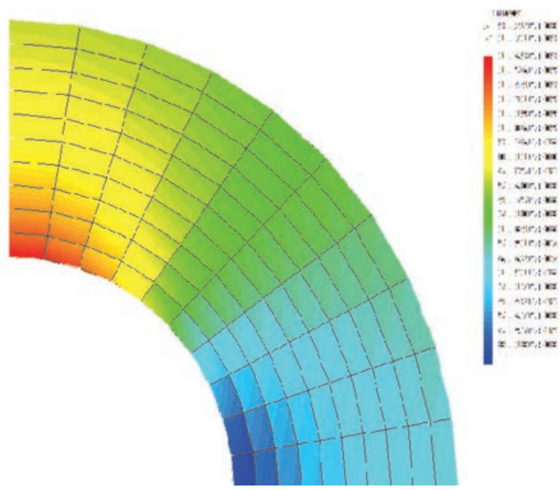

Figure 12. Discretisation of cylinder

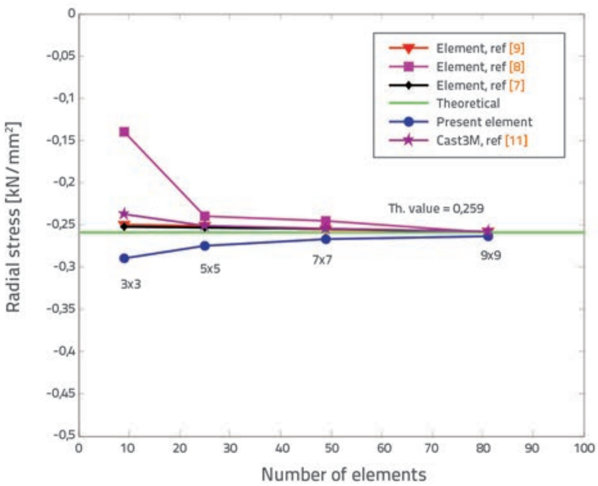

Figure 10. Convergence of σ_r at *r* = 30 mm

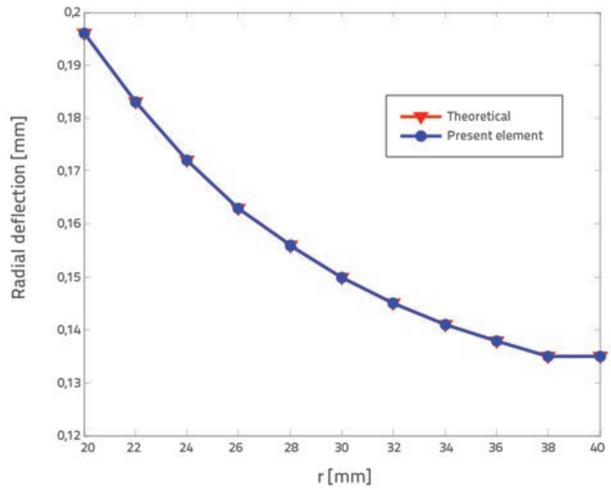

Figure 13. Variation of *u* under internal pressure

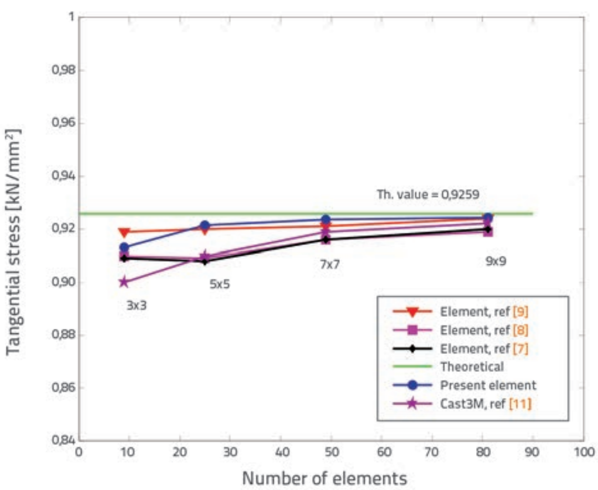

Figure 11. Convergence of σ_θ at *r* = 30 mm

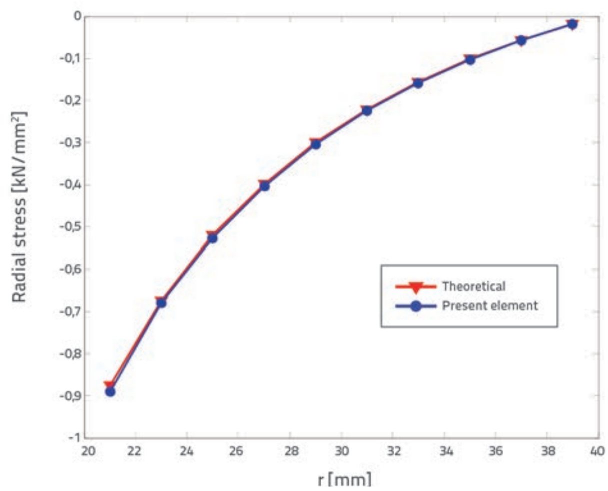

Figure 14. Variation of σ_r under internal pressure

The analysis was performed for the cylinder discretized by increasing the number of finite elements. An example is shown in Figure 12.

These figures show that convergence to the exact solution is obtained even when a coarse mesh is used. This illustrates a high degree of accuracy obtained from others elements.

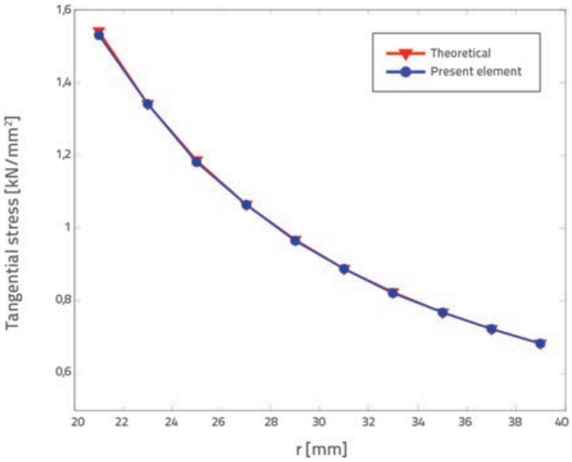

Figure 15. Variation of σ_θ under internal pressure

4.2.2. Cylinder under temperature only

Figures 16, 17, and 18 give convergence curves of radial deflection, the radial and tangential stress at r = 30 mm of the cylinder under temperature, as compared with theoretical values given by Timoshenko [10]. It can be seen that the present element gives good results.

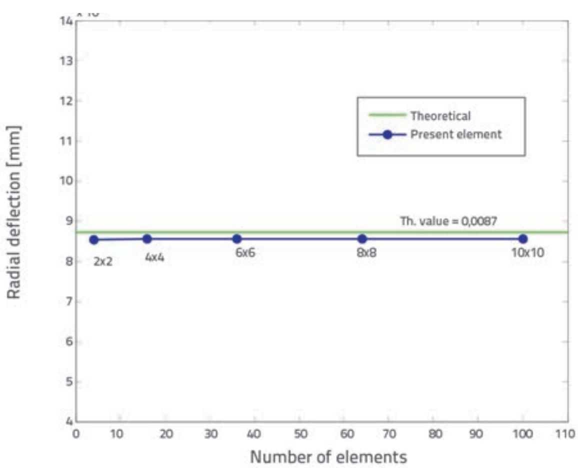

Figure 16. Convergence of u at r = 30 mm

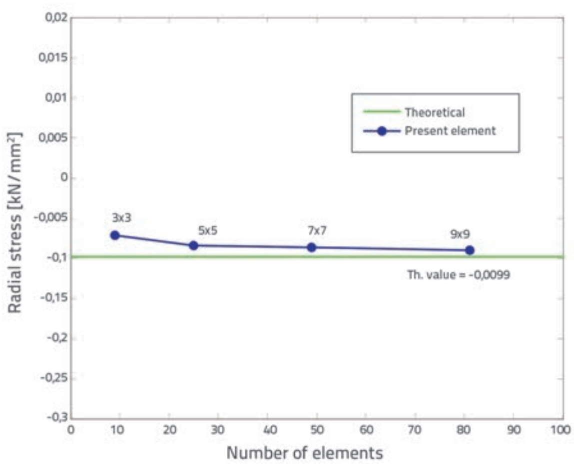

Figure 17. Convergence of σ_r at r = 30 mm

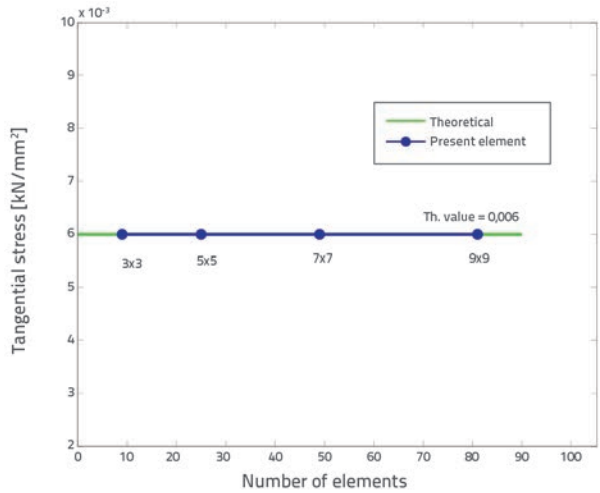

Figure 18. Convergence of σ_θ at r = 30 mm

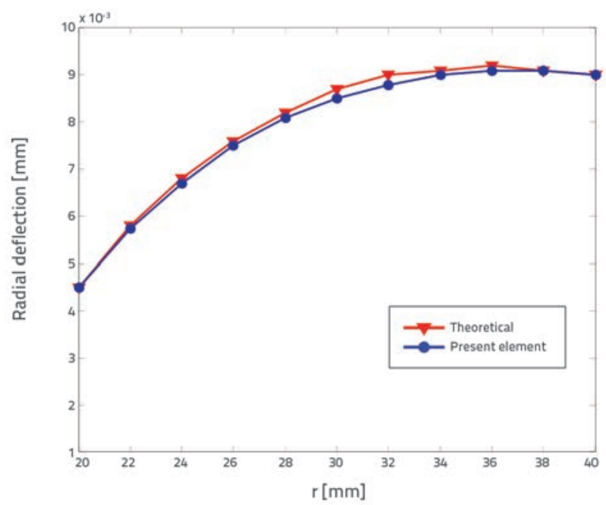

Figure 19. Variation of u under temperature loading

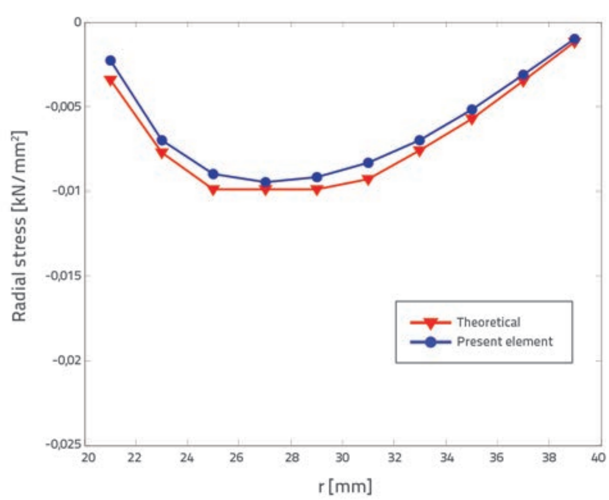

Figure 20. Variation of σ_r under temperature loading

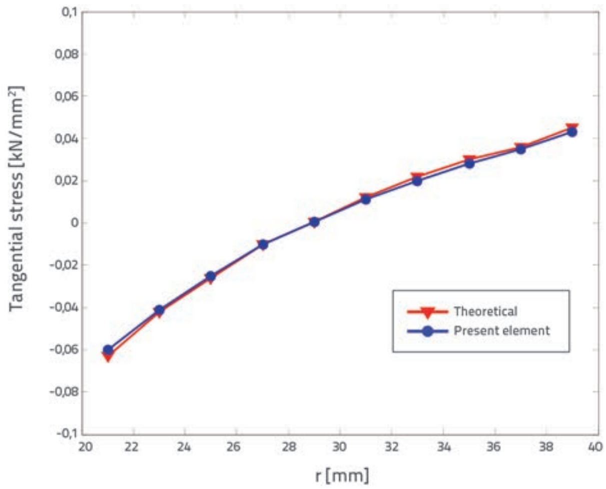

Figure 21. Variation of σ_θ under temperature gradient

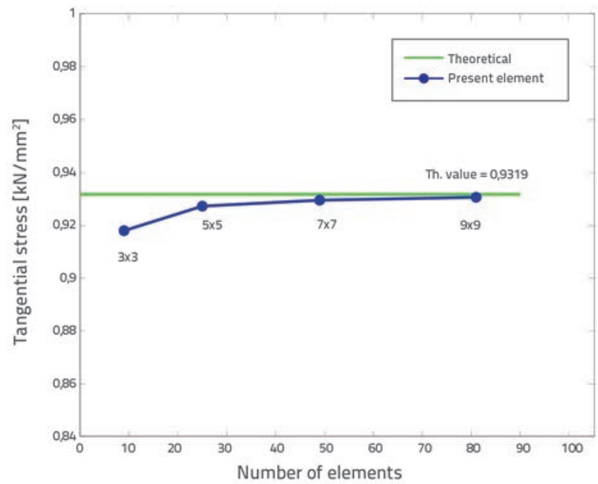

Figure 24. Convergence of σ_θ at r = 30 mm

4.2.3. Cylinder under combined loading (pressure and temperature)

Figures 22, 23, and 24 give convergence curves of radial deflection, the radial and tangential stress at r = 30 mm.

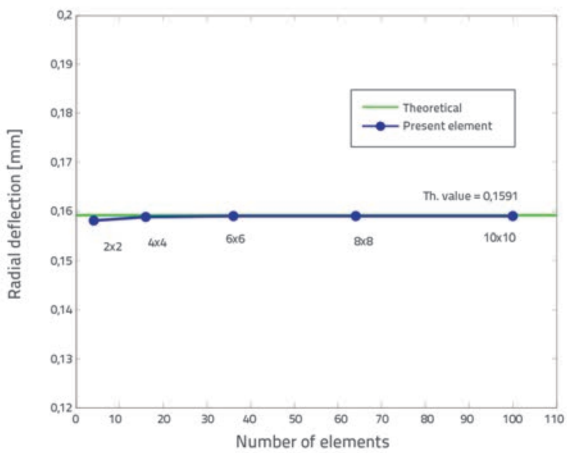

Figure 22. Convergence of u at r = 30 mm

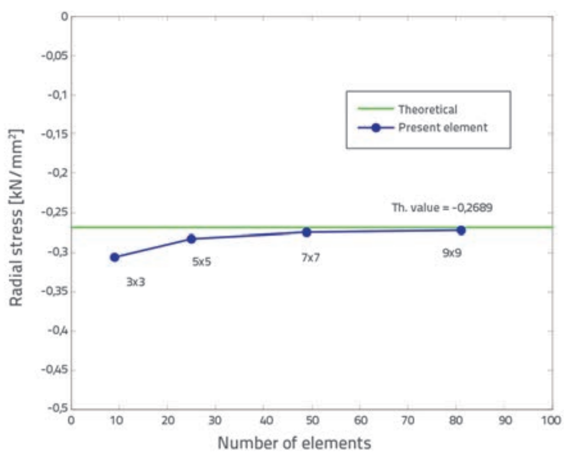

Figure 23. Convergence of σ_r at r = 30 mm

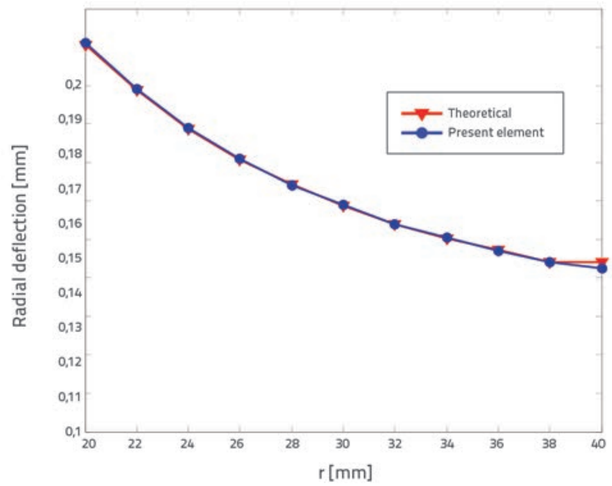

Figure 25. Variation of u under pressure and temperature

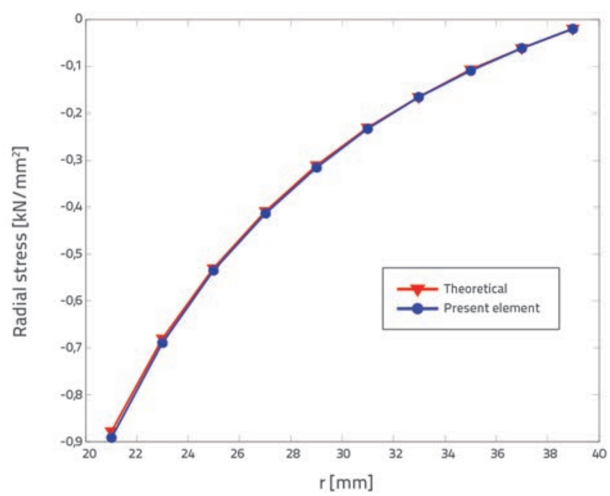

Figure 26. Variation of σ_r under pressure and temperature

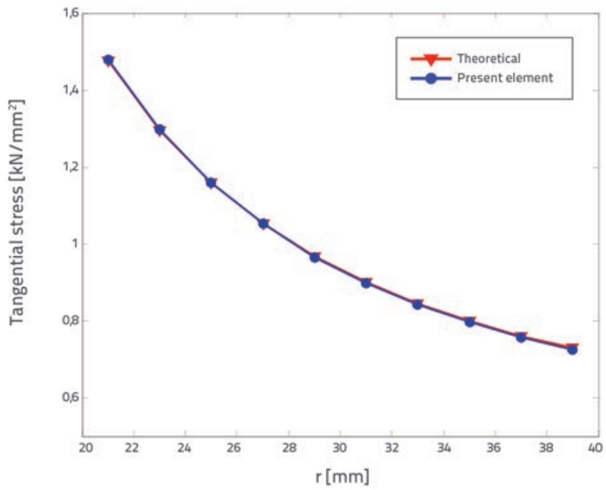

Figure 27. Variation of σ_θ under pressure and temperature

5. Conclusion

In this paper, the strain based finite element is used to develop a sector element in the system of polar coordinates with two translational degrees of freedoms, as well as the inplane drilling rotation. This element can predict the stress and displacement at any point of the cylinder subjected to combined pressure and temperature. Numerical results of the analysis, compared with theoretical ones and values obtained by other elements and commercial software, show a good performance of this element, with a great economy of computing and reduced programming effort.

Appendix

Components of the matrix [*C*] of this element are:

$$[C]=\begin{bmatrix}
\cos\beta & \sin\beta & 0 & r_1 & 0 & r_1^2+1 & 0 & 0 & 0 & \beta r_1+1 & r_1^3 & 0 \\
-\sin\beta & \cos\beta & r_1 & -\beta r_1 & \beta r_1 & -\beta & r_1\log(r_1) & -\frac{\beta^2 r_1^4}{6} & \frac{r_1\beta^2}{2} & -\beta-r_1\,log(r_1)-\frac{\beta^2 r_1}{2} & 1 & -2r_1^2 \\
0 & 0 & 1 & -\beta & \beta & -\beta/2r_1 & 1/2+\log(r_1) & -\frac{5\beta^2 r_1^3}{12} & \beta & -1-\frac{\beta^2}{2}-\log(r_1)-\frac{\beta}{2r_1} & 1 & -3r_1 \\
\cos\beta & -\sin\beta & 0 & r_1 & 0 & r_1^2+1 & 0 & 0 & 0 & -\beta r_1+1 & r_1^3 & 0 \\
\sin\beta & \cos\beta & r_1 & \beta r_1 & -\beta r_1 & \beta & r_1\log(r_1) & -\frac{\beta^2 r_1^4}{6} & \frac{r_1\beta^2}{4} & \beta-r_1\log(r_1)-\frac{\beta^2 r_1}{2} & 1 & -2r_1^2 \\
0 & 0 & 1 & \beta & -\beta & \frac{\beta}{2r_1} & \frac{1}{2}+\log(r_1) & -5\beta^2 r_1^3 & \frac{\beta^2}{4} & -1-\frac{\beta^2}{2}-\log(r_1)+\frac{\beta}{2r_1} & 1 & -3r_1 \\
\cos\beta & \sin\beta & 0 & r_2 & 0 & r_2^2+1 & 0 & 0 & 0 & \beta r_2+1 & r_2^3 & 0 \\
-\sin\beta & \cos\beta & r_2 & -\beta r_2 & \beta r_2 & -\beta & r_2\log(r_2) & -\frac{\beta^2 r_2^4}{6} & \frac{r_2\beta^2}{4} & -\beta-r_2\log(r_2)-\frac{\beta^2 r_2}{2} & 1 & -2r_2^2 \\
0 & 0 & 1 & -\beta & \beta & -\frac{\beta}{2r_2} & \frac{1}{2}+\log(r_2) & -5\beta^2 r_2^3 & \frac{\beta^2}{4} & -1-\frac{\beta^2}{2}-\log(r_2)-\frac{\beta}{2r_2} & 1 & -3r_2 \\
\cos\beta & -\sin\beta & 0 & r_2 & 0 & r_2^2+1 & 0 & 0 & 0 & -\beta r_2+1 & r_2^3 & 0 \\
\sin\beta & \cos\beta & r_2 & \beta r_2 & -\beta r_2 & \beta & r_2\log(r_2) & -\frac{\beta^2 r_2^4}{6} & \frac{r_2\beta^2}{2} & \beta-r_2\log(r_2)-\frac{\beta^2 r_2}{2} & 1 & -2r_2^2 \\
0 & 0 & 1 & \beta & -\beta & \beta/2r_2 & \frac{1}{2}+\log(r_2) & -\frac{5\beta^2 r_2^3}{12} & -\beta & -1-\frac{\beta^2}{2}-\log(r_2)+\frac{\beta}{2r_2} & 1 & -3r_2
\end{bmatrix}$$

REFERENCES

[1] Rebiai, C., Belounar, L.: A new strain based rectangular finite element with drilling rotation for linear and nonlinear analysis, Archives of Civil and Mechanical Engineering, 13 (2013) 1, pp. 72–81.

[2] Djoudi, M.S., Bahai, H.: Strain based finite element for the vibration of cylindrical panels with opening, Thin-Walled Structures, 42 (2004) 4, pp. 575–588.

[3] Himeur, M., Guenfoud, M.: Bending triangular finite element with a fictious fourth node based on the strain approach, European Journal of Computational Mechanics, 20 (2012) 7-8, pp. 455-485.

[4] Ergatoudis, I., Irons, B. M., Zienkiewicz, O.C.: Curved isoparametric quadrilateral element for finite element analysis, International journal of solids and structures, 4 (1968) 1, pp. 31-42.

[5] Raju, I.S., Rao, A.K.: Stiffness matrices for sector element, A.I.A.A. J., 7 (1969) 1, pp.156-157.

[6] Sabir, A.B., Sfendij, A.: Finite element for plane elasticity problems, Proceeding of conference femcad crash, Institute for industrial technology transfer, Paris, pp.137-144, 1993.

[7] Sabir, A.B., Salhi, H.Y.: A strain based finite element for general plane elasticity in polar coordinates, Res. mechanica, 19(1986) 1, pp. 1-16.

[8] Sabir, A.B., Djoudi, M.S.: A sector in plane finite element with a rotational degree of freedom, proceeding of the 5th International conference of the structural engineering. Technology Transfert series, pp. 55-62, 1990.

[9] Bouzrira, C., Sabir, A.B., Nemouchi, Z.: A sector inplane finite element in polar coordinates with rotational degree of freedom, Archives of civil engineering, LI (2005) 4, pp. 471-483.

[10] Timoshenko, S., Goodier, J. N.: Theory of elasticity, Third edition, Mc Graw Hill, New York, 1951.

[11] Cast3M, *www-cast3m.cea.fr*